S Al-Khatib
A Berradja
J-P Celis
G Willems

In vitro friction of stainless steel arch wire–bracket combinations in air and different aqueous solutions

Authors' affiliations:
Shadi Al-Khatib, Guy Willems, Department of Orthodontics, School of Dentistry, Oral Pathology and Maxillofacial Surgery, Katholieke Universiteit Leuven, Leuven, Belgium
Abdenacer Berradja, Jean-Pierre Celis, Department of Metallurgy and Materials Engineering (MTM), Katholieke Universiteit Leuven, Leuven, Belgium

Correspondence to:
Dr Guy Willems
Department of Orthodontics
Faculty of Medicine, School of Dentistry, Oral Pathology and Maxillofacial Surgery
Katholieke Universiteit Leuven
Kapucijnenvoer 7
B-3000 Leuven
Belgium
Tel.: +32 16 332459
Fax: +32 16 332435
E-mail: guy.willems@med.kuleuven.ac.be

Structured Abstract
Authors – Al-Khatib S, Berradja A, Celis J-P, Willems G.
Objectives – To investigate the *in vitro* coefficient of friction of stainless steel arch wire–bracket combinations under fretting contact test conditions performed in air and in different aqueous solutions, like Ringer solution, Ringer with addition of a buffer, Ringer with addition of glucose, and Coca Cola®.
Methods – The fretting test set-up used allowed to control on-line the contact configuration and the positioning of the contacting parts. A specific positioning method was used to achieve a parallel alignment of arch wire and bracket slot. The effect of arch wire size, roughness, and test environment were investigated.
Results – It was found that the aqueous solutions act as a lubricant compared to air. Friction was affected by the arch wire width while the roughness was found to have a limited effect. Stainless steel 0.018″ × 0.025″ arch wires exhibited higher frictional forces than stainless steel 0.017″ × 0.025″ arch wires on sliding against stainless steel 0.018″ × 0.025″ brackets in the selected test environments when tested under identical fretting test conditions. The wear damage on the arch wire after these *in-vitro* fretting tests was investigated. It revealed that these *in-vitro* tests are governed by a competition between oxidational wear and abrasive wear taking place at contact areas between brackets and arch wires.
Conclusions – For all aqueous solutions a lower coefficient of friction was found compared to tests performed in ambient air.

Key words: arch wire; brackets; buffer; Coca Cola®; corrosion; dry conditions; fretting; friction; glucose; orthodontic materials; ringer solution; stainless steel; wear; wet conditions

Dates:
Accepted 4 March 2005

To cite this article:
Orthod Craniofacial Res **8**, 2005; 96–105
Al-Khatib S, Berradja A, Celis J-P, Willems G:
In vitro friction of stainless steel arch wire–bracket combinations in air and different aqueous solutions

Introduction

The investigation in laboratory tests of the friction between numerous types of brackets and arch wires has been frequently reported in literature (1–4). Various *in-vitro* techniques were used to describe the frictional behavior of arch wire–bracket combinations. Techniques such as dynamometer or a weight bucket have been used (2). Recently, a lot of research was also performed to simulate clinical conditions by using different technologies and media (3).

In the last decade, the most frequently used *in-vitro* test set-up was the one developed by Kusy and Whitley (4). These authors used a standardized universal testing machine (Instron Model TTCM; Instron Corporation, Canton, MA, USA) to investigate friction between brackets and arch wires under different environmental and mechanical conditions. That technique is based on a unidirectional single linear sliding motion between brackets and arch wires. However, experimental data were not acquired on-line and the dynamics of the clinical frictional process was not considered (5).

In a recent work (6), an *in-vitro* fretting test set-up operating under reciprocating tangential displacements or fretting conditions was proposed. That device was used to investigate the frictional behavior of arch wire–bracket combinations in dry test conditions. That machine allows an on-line control of mechanical parameters such as normal force, displacement amplitude, contact sliding frequency, tangential force, and dissipated energy generated during fretting tests between bracket and arch wire surfaces. The role of these test parameters was reviewed by Waterhouse (7) and he described fretting phenomena in vibrating pair material contacts.

Furthermore, friction on orthodontic arch wire–bracket combinations was reported to be affected by factors such as type of arch wire and bracket materials (8), their size and shape (9), width and slot dimensions (10), the surface composition, roughness and cleanliness of the contacting surfaces (11), the bracket-to-arch wire positioning in a three-dimensional space (12), the ligature force (13), and the type of ligation (14) and inter-bracket distances (15). An important factor controlling the frictional force between brackets and arch wires is saliva (16). In the presence of human saliva or artificial saliva (17), significant differences in friction were noticed between dry and wet test conditions (18–21). Some researchers relate the effect of saliva on friction to the 'adhesion theory of friction' (22). Accordingly, an increase in friction in the presence of polar liquids, such as artificial saliva, generates an increased atomic attraction between ionic species. This leads to the adhesion between surface asperities at the bracket–arch wire interface, which may enhance the resistance to sliding. Such a behavior was observed in the case of stainless steel and nickel-titanium arch wires (23). Other authors reported that the effect of saliva on friction mainly depends on the loading conditions (24,25). At low forces, saliva acts as a lubricant while at high forces, friction may increase because saliva is expelled from the contacts between bracket and arch wire. As a consequence of metal-to-metal contacts, the shear resistance to sliding increases.

The studies reported in literature differ frequently in tested materials, methodology of the experimental design, recording technique, and lubricants used. It is then difficult to compare results and this may well explain some inconsistence in the results. It is a fact that it is difficult to simulate clinical conditions in laboratory tests.

This research aims at investigating the *in-vitro* frictional resistance of stainless steel arch wire–bracket combinations under fretting contact conditions. Clinical conditions were simulated by using four different media, namely a Ringer solution as artificial saliva, Ringer solution containing a buffer, a Ringer solution containing glucose, and Coca Cola®.

Materials and methods

The fretting machine used was developed at the Department of Metallurgy and Materials Engineering, Katholieke Universiteit Leuven (Belgium). It was described earlier (6) and was used to investigate the frictional behavior of arch wire–bracket combinations tested in dry and different wet environments.

Stainless steel orthodontic rectangular arch wires (3M Unitek, Monrovia, CA, USA) with two different cross-sections, namely 0.017″ × 0.025″ and 0.018″ × 0.025″, were evaluated in contact with stainless steel brackets (Mini Twin; 3M Unitek) with a 0.018″ × 0.025″ slot size.

The chemical composition, the initial appearance, and the surface roughness of each arch wire were investigated by EDAX analyses (energy dispersive X-ray) and scanning electron microscopy (SEM; Philips XL30 FEG; Philips, Eindhoven, The Netherlands). Roughness was determined with a Rank Taylor Hobson profilometer, as described by Willems *et al.* (26). The

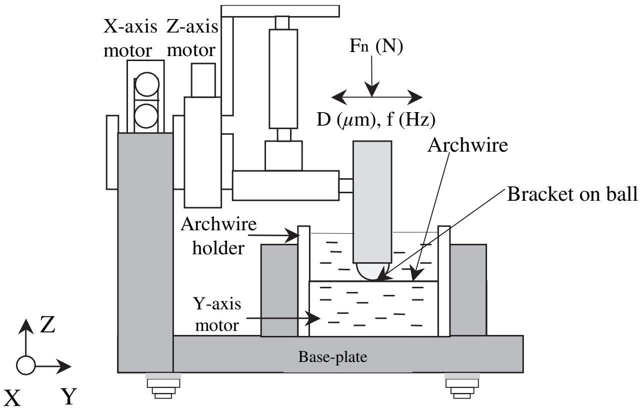

Fig. 1. *In vitro* set-up of MTM fretting machine for tests performed in aqueous solutions. Metallic wire is mounted on polymer wire holder (PWH), especially designed for testing in aqueous solutions.

Table 1. **Specification of solutions used in this study**

	Composition		
Solution	Compound	Weight	pH
Ringer	NaCl	4.201 g	6.6
	KCl	0.151 g	
	$CaCl_2$	0.149 g	
	H_2O	0.5 L	
Ringer + buffer	NaCl	4.201 g	7.9
	KCl	0.151 g	
	$CaCl_2$	0.149 g	
	H_2O	0.5 L	
	$NaHCO_3$	0.104 g	
Ringer + glucose	NaCl	4.201 g	5.67
	KCl	0.151 g	
	$CaCl_2$	0.149 g	
	H_2O	0.5 L	
	Glucose	0.513 g	
Coca Cola	–	–	2.8

surface morphology of the tested arch wires was also examined by SEM and EDAX for possible wear and possible formation of wear debris (called third body) or corrosion products.

The stainless steel arch wires were aligned according to the centered positioning method (6), and were subjected to a small displacement oscillatory sliding (fretting). Brackets glued on top of chromium-steel balls (100 Cr 6; Fritsch GmbH, Idar. Oberstein, Germany) with a diameter of 10 mm, were used as counterbody and loaded on top of the arch wires.

The fretting experiments were performed using either metallic (MWH) or polymer wire holders (PWH) (Fig. 1) for tests performed in ambient air of 50% RH or immersed in solutions, respectively. The tested solutions were: Ringer solution selected as a model of body fluid (27), a Ringer solution containing a buffer to get a stable pH value, a Ringer solution containing glucose chosen for its incidence effect on dental caries (28), and finally, Coca Cola® to evaluate the effect of acidity on arch wire–bracket friction. The chemical compositions and pH values of the considered solutions are given in Table 1.

The arch wires were fixed at their two ends in the sample holder mounted on the oscillating *x–y* table. The bracket was loaded on top of the rectangular arch wire at a normal force of 2 N. This normal force corresponds to the force applied by an elastic module when tightening the arch wire into a bracket slot (6). Applying a vertical force significantly simplifies the clamping of the arch wires in the brackets, and allows a standardization of the test set-up by eliminating the need for fixing arch wires to brackets with elastic or metallic ligatures. A linear displacement amplitude of 200 μm at a vibrating frequency of 1 Hz was applied. These fretting tests were performed for 20 cycles at 23°C. Each set of test conditions was repeated 10 times. The mechanical contact response was monitored on-line by measuring frictional force vs. displacement hysteresis loops (Fig. 2). The dynamic frictional force and the dissipated friction energy were calculated from these hysteresis loops along with their standard deviations. The coefficient of friction was calculated from the ratio of the dynamic frictional force to the applied normal force. The cumulative dissipated energy was obtained by integrating the area of the tangential force vs. displacement loops of each individual fretting cycle over the test period (18). Changes in friction during the test duration are implicitly incorporated in the cumulative dissipated energy.

Prior to the tests, bracket slots and arch wires were cleaned with ethanol (naturalized ethanol + 5% diethyl ether), and dried with warm air.

Besides the control of the mechanical parameters during the sliding tests, electrochemical noise measurements were recorded during fretting tests performed in the solutions. Hereto an electrochemical potentiostat interface (Solartron, type 1287; Braine L'Alleud, Belgium) was used (Fig. 3). These electro-

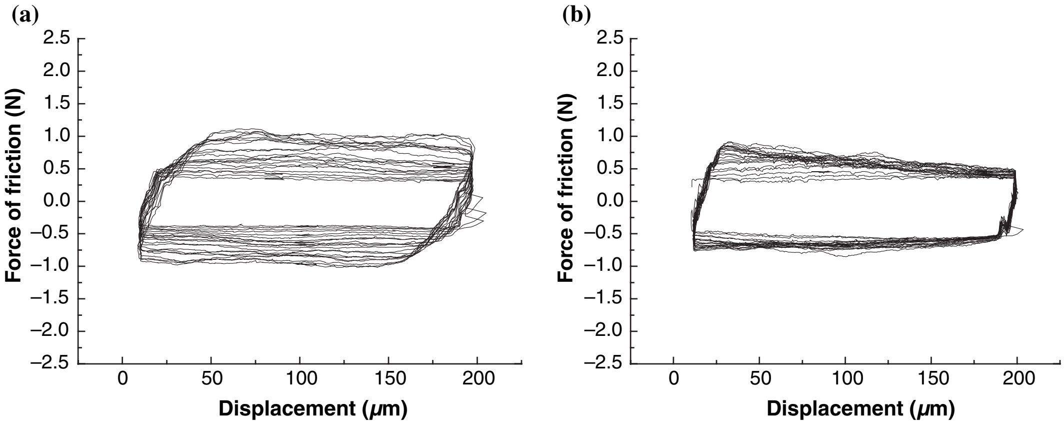

Fig. 2. Frictional force-displacement loops recorded on-line during fretting tests performed on 0.017″ × 0.025″ stainless steel arch wire–bracket combinations. Test conditions were: (a) ambient air of 50% RH and (b) Ringer solution. The integrated surface corresponds to the dissipated energy.

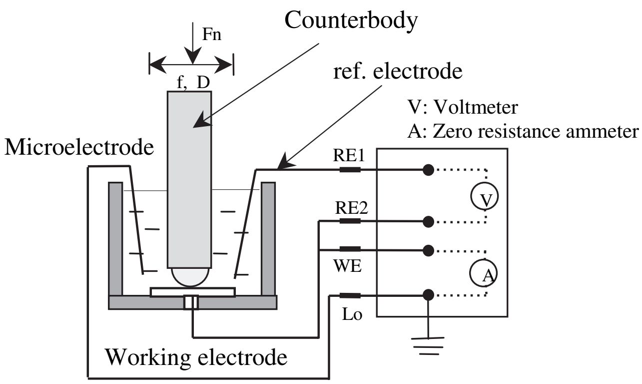

Fig. 3. Schematic drawing of electrochemical noise measurement technique connected to the fretting machine.

chemical data on potential and current allow a better understanding of the possible depassivation (removal of oxide surface film) and repassivation (growth of oxide surface film) phenomena taking place during the sliding between brackets and arch wires. Prior to the fretting tests, the arch wire–bracket combinations were dipped in the test solution for approximately 400 s in order to get a stable potential. A stable potential reflects a stable arch wire surface condition.

The statistical analysis of the data obtained from the fretting tests were performed using the ANOVA general linear model procedure of the SAS statistical package (SAS Institute, Cary, NC, USA) performing a Tuckey's studentized range test for the variable coefficient of friction (COF). The ANOVA enabled to differentiate significant statistical differences between test set-ups and the coefficient of friction for the evaluated arch wires. The minimum level of significance was set at 0.05.

Results

Tables 2a and b depict the results from the SEM–EDAX analyses of the unused arch wires as well as the roughness values of these arch wires. From these results it seems that the alloy used here for the production of the evaluated stainless steel arch wires is AISI type 304 (29).

The PWH set-up was used to evaluate the frictional behavior of arch wire–bracket combinations in air and immersed in different aqueous solutions. In order to validate this sample holder set-up, similar experiments in ambient air of 50% RH were carried out with the MWH. Both MWH and PWH set ups provide comparable results in terms of coefficient of friction. The obtained results were in agreement with the previously reported data in which this MWH set-up was used (6).

Table 2a. **Chemical analyses of the stainless steel 3M orthodontic arch wires 0.017″ × 0.025″ and 0.018″ × 0.025″ investigated in this study**

Main elements	Fe	Cr	Ni	O	C	Al	Mn	Si
Wt%	70.85	18.7	9.3	–	0.11	–	0.02	1.13

Table 2b. **Mean roughness values of 0.017″ × 0.025″ and 0.018″ × 0.025″ as-delivered stainless steel arch wires (3M)**

Type of arch wire	R_a	R_t	R_{sk}	R_{ku}	R_{zISO}	R_{zDIN}
0.017″ × 0.025″	0.02	0.35	−0.2	6.17	0.13	0.18
0.018″ × 0.025″	0.02	0.375	−0.62	7.53	0.12	0.18

The data from on-line mechanical contact measurements were evaluated for the stainless steel arch wire–bracket combinations during fretting performed under different environmental test conditions. The typical obtained data for 0.017″ × 0.025″ stainless steel arch wires are plotted as tangential force vs. displacement amplitude hysteresis loops in Fig. 2a,b for tests performed in ambient air of 50% RH and in Ringer solution, respectively. The area enclosed by the force–displacement hysteresis loop represents the friction energy dissipated in the contact during the corresponding fretting cycle. At the onset of each stroke, the lateral slope in the frictional force reflects the combined elastic deformation of bracket and arch wire surfaces, and the stiffness of the tribometer. The presence of a plateau in the frictional force indicates a gross slip between the two contacting bodies, i.e. bracket and arch wire. It was observed from these figures that the largest loop (highest dissipated energy) was acquired for tests performed in ambient air while the smallest one (lowest dissipated energy) is recorded in the Ringer solution. The corresponding typical evolution of the dynamic frictional force with test duration is shown in Fig. 4a,b for tests performed in ambient air of 50% RH and Ringer solution, respectively. During the first runs of a test, the frictional force rises up to a constant value. This increase in frictional force at the onset of the test is a running-in phenomenon. Therefore, the statistical analysis of the dynamic frictional force was quantified using values from only the last 7 cycles where the frictional force remains constant.

The variation of the COF and its standard deviation (SD) during fretting for the different arch wire–bracket combinations tested under different environmental test conditions and different sample holder set-ups, are presented in Fig. 5. The ANOVA statistical procedure reveals a significant difference. The results of the Tukey's range test demonstrate significant differences in the coefficient of friction for the 0.017″ × 0.025″ and 0.018″ × 0.025″ arch wires. The highest frictional force among the two arch wires was noticed with the 0.018″ × 0.025″ arch wire during tests done in ambient air, while the lowest frictional force was recorded in the Ringer solution. For example, the 0.017″ × 0.025″ and 0.018″ × 0.025″ stainless steel arch wires exhibit both a coefficient of friction that was significantly different for tests performed in ambient air and in aqueous solutions, i.e. the Ringer's solutions and Coca Cola®.

Roughness measurements on the different arch wires before the tests (Table 2a,b) showed that R_a values for both 0.017″ × 0.025″ and 0.018″ × 0.025″ arch wires were equal. The only difference was noticed in the skewness value R_{sk}. That is the measure of symmetry of the profile across a mean line through the roughness of the arch wires. The 0.018″ × 0.025″ arch wire has a higher skewness than the 0.017″ × 0.025″ arch wire (Table 2a,b).

Representative SEM micrographs for stainless steel 0.017″ × 0.025″ arch wires before fretting are shown in Fig. 6a,b. Similar micrographs were obtained for stainless steel 0.018″ × 0.025″ arch wires. In general, in both cases few scratches and grooves are noticed on the surface of both arch wires resulting probably from the arch wire drawing process. Figure 7a,b shows the wear tracks on stainless steel 0.017″ × 0.025″ arch wires after fretting test performed in ambient air. The SEM micrographs reveal abrasive wear scratches in addition to larger scratches and grooves. Figure 8a,b shows SEM

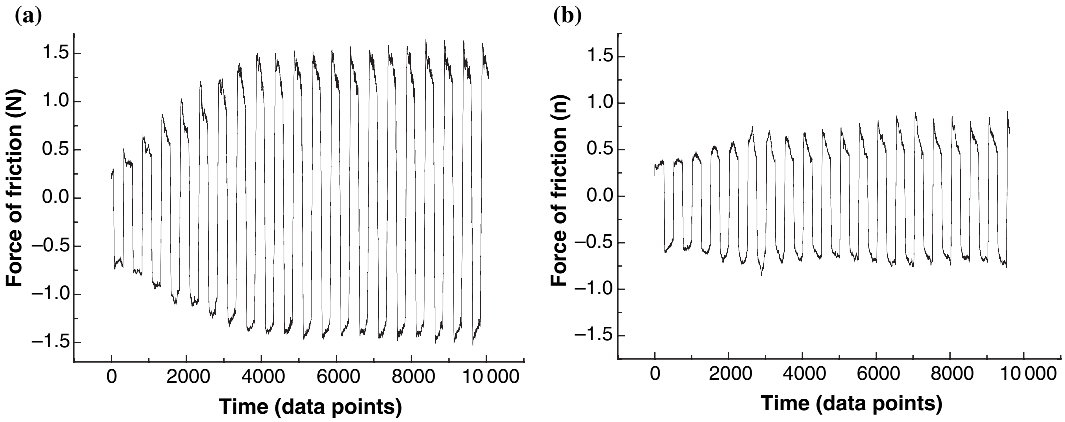

Fig. 4. Typical force–time graphs illustrating the running-in phenomenon for 0.017″ × 0.025″ stainless steel arch wire–bracket combinations. Tests were performed (a) in ambient air of 50% RH and (b) in Ringer solution.

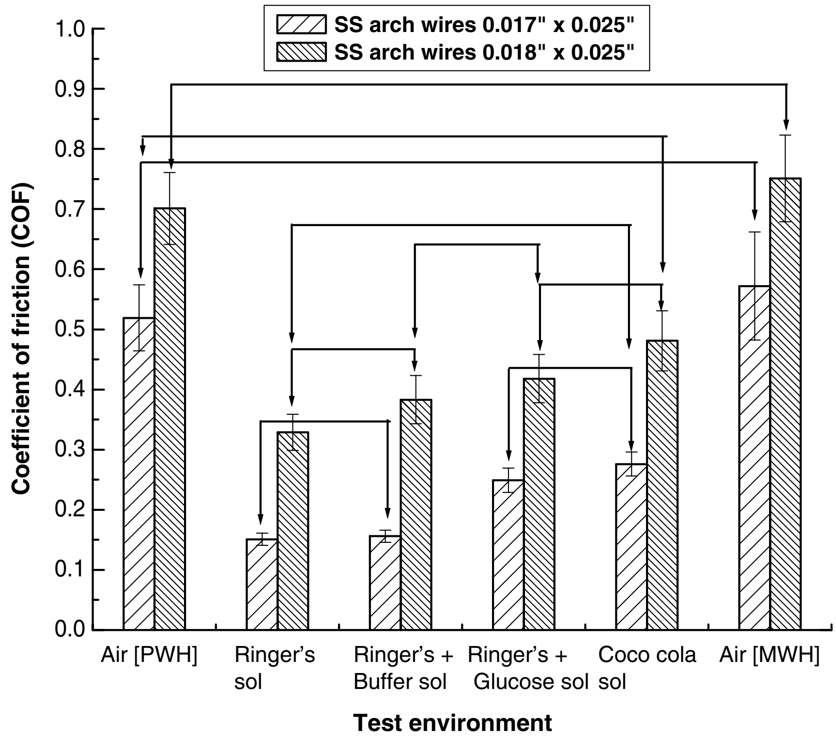

Fig. 5. Coefficients of friction and standard deviations recorded on 0.017″ × 0.025″ and 0.018″ × 0.025″ stainless steel arch wires during fretting tests performed in air and different solutions. Vertical bars represent the standard deviation based on results of 10 experiments. Horizontal lines above the bars show the results that are not statistically different.

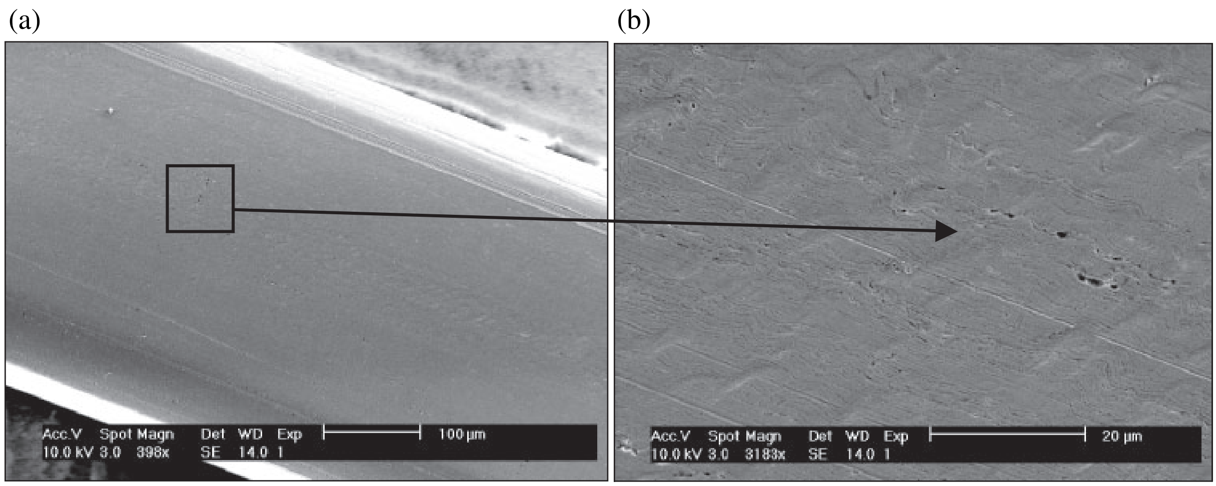

Fig. 6. SEM micrographs of unused 0.017″ × 0.025″ stainless steel arch wire at different magnification. (a) General view of arch wire surface, (b) detail of the surface showing irregular surface finish probably due to the drawing process during manufacturing.

micrographs of the wear track obtained on stainless steel 0.017″ × 0.025″ arch wire after fretting test in the Ringer solution. All the micrographs show abrasive wear scratches, large scratches, and grooves, and debris.

Electrochemical noise measurements were performed before, during and after sliding tests. In this way, changes in the surface state can be implicitly correlated with changes in potential and current noises. Typical potential–current vs. time plots are shown in Fig. 9 for stainless steel 0.017″ × 0.025″ arch wires sliding against a stainless steel 0.018″ × 0.025″ bracket in a Ringer solution. Before starting the fretting process, a steady-state current and potential were observed. On loading the bracket on the arch wire, the potential undergoes a significant negative shift of about 0.6 V while the current rises in the positive direction by about 1.1 μA. After this running-in phase that extends for about 100 s, the fretting test was started for a duration of 20 s. During fretting, both potential and current fluctuate in phase. Both potential and current

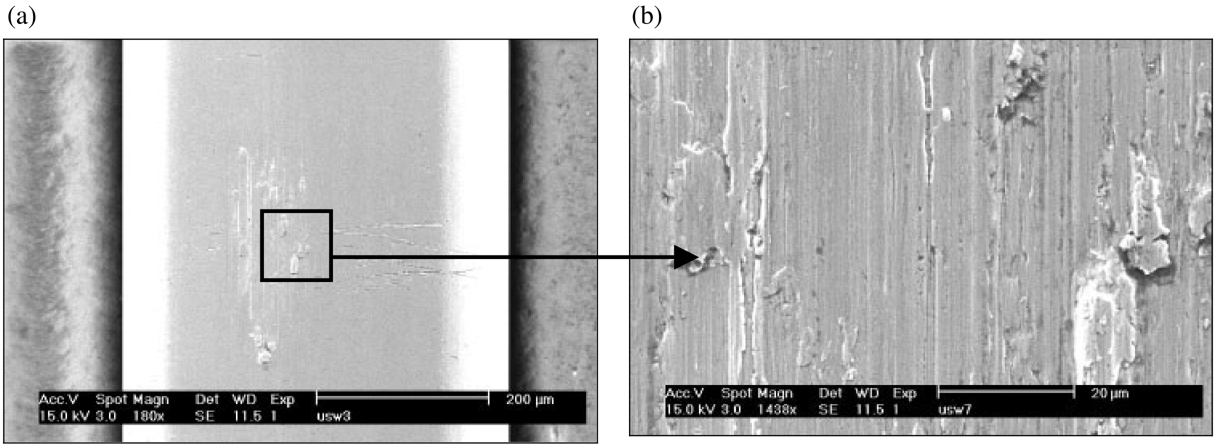

Fig. 7. SEM micrographs after fretting tests performed in ambient air of 0.017″ × 0.025″stainless steel arch wire. Fretting test parameters were: 2 N, 1 Hz, 200 μm, 20 cycles, 23°C. Fretting tests were performed with bracket 0.018″ × 0.025″. (a) General view of the wear track, (b) details of the wear track showing scratches due to abrasive wear.

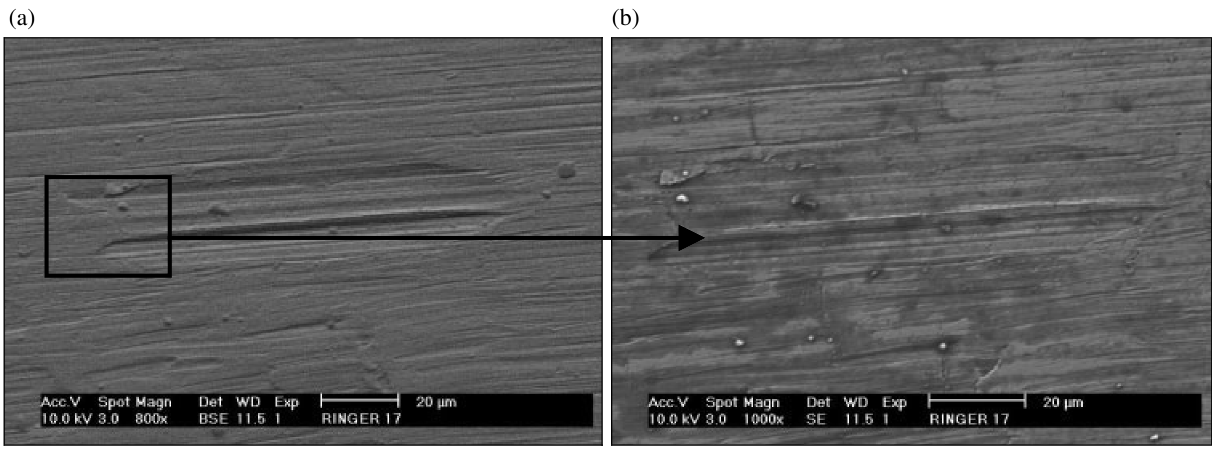

Fig. 8. SEM micrographs taken after fretting tests in a Ringer solution on stainless steel arch wires 0.018″ × 0.025″. Fretting test parameters were: 2 N, 1 Hz, 200 μm, 20 cycles, 23°C. Fretting tests were performed with bracket 0.018″ × 0.025″. (a) General view of the wear track, (b) details of the wear track showing scratches due to abrasive wear.

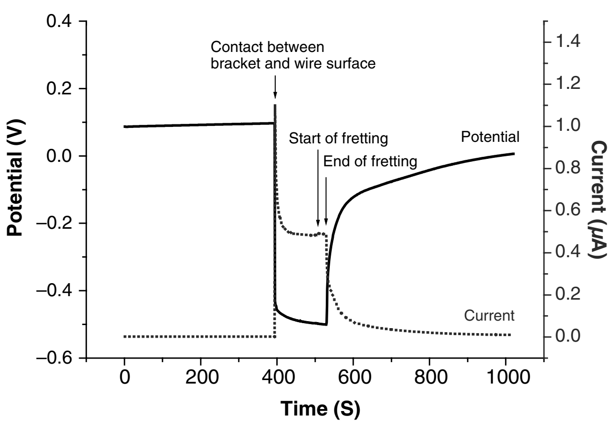

Fig. 9. Evolution of potential and current noise recorded on stainless steel arch wires 0.017″ × 0.025″ before, during, and after fretting tests performed in a Ringer solution. Fretting test were parameters: 2 N, 1 Hz, 200 μm, 20 cycles, 23°C.

remain in this state as long as the fretting test was performed. At the end of the fretting tests, the bracket was lifted away from the arch wire. At that time, the potential of the arch wire increases progressively but reaches a level lower than before the start of the fretting test. The current flowing between the arch wire and a microelectrode (Pt micro-cathode) used as counter-electrode, decreases drastically reaching almost the initial current value recorded before fretting.

Discussion

A sliding test was used to evaluate the friction between different stainless steel arch wires in contact with a stainless steel bracket. An MWH was used for tests in ambient air and PWH was used for tests performed in ambient air or immersed in different solutions. No significant statistical differences were found between sliding tests performed in ambient air with the PWH developed for this work and the ones performed with a previously used MWH (6). The test consisted of an oscillating sliding at a small displacement amplitude (fretting) between bracket and arch wire. This set-up was chosen because tooth movement is not a linear and continuous motion but a discontinuous and dynamic one (6).

After calibration of the PWH, the effect of four different media was evaluated in order to simulate the *in-vivo* conditions. It was found that under wet testing conditions, i.e. in Ringer's solutions and Coca Cola®, a decrease of the coefficient of friction was noticed compared to test in ambient air. This could be attributed to a lubrication effect of these aqueous solutions or to the presence of a third-body at the interface between bracket and arch wire. That third-body may be wear debris or corrosion products which may alter the initial friction contact conditions. This funding is in agreement with earlier reports (24,25) for a similar tribosystem but involving lower normal loads. In fact, friction between sliding surfaces is a result of various synergistic effects of adhesion between surfaces, wear particles formation and movement, and elastic or plastic asperity deformation. This friction usually causes some wear. For instance, wear particles can remain entrapped in the sliding interface and undergo a repeated deformation resulting in the consumption of energy. In aqueous solutions, such wear particles may act as a lubricant resulting in a lower energy consumption and thus contribute to a decrease of the coefficient of friction. In addition, fretting in aqueous solutions may generate corrosion products and oxidize or hydrolyze material surfaces present in the sliding interface. Such corrosion products can be formed by electrochemical oxidation reactions. Depending on the fretting conditions and the nature of the interface, the oxide layer and the corrosion products on the top of material surfaces can be destroyed (depassivation process) during the sliding contact events, and the bare material surfaces may re-oxidize (repassivation process) after the depassivating contact event. Depending on the nature of the repassivated surface film (abrasive oxide or lubricating oxide), the frictional force may increase or decrease. In this study, the frictional force was found to be lower in fretting tests performed in solutions compared to tests performed in ambient air. However, during the running-in phase (the first 13 cycles) (Fig. 4), it was noticed that the frictional force increases gradually till reaching a stable value for the different arch wire–bracket combinations. This increase may be attributed to an initial abrasive contact between bracket and arch wire, or a minimum dissipation of frictional energy required for the formation of wear debris.

The highest coefficient of friction was noticed for the 0.018″ × 0.025″ arch wire sliding against a 0.018″ × 0.025″ slot bracket in all test environments used in this study. The lowest coefficient of friction was recorded for 0.017″ × 0.025″ arch wire (Fig. 5). It seems thus that the dimensions of the arch wire play a role in the friction behavior of arch wire–bracket combinations. The contact area between the bracket and the arch wire surface is the largest one in case of 0.018″ × 0.025″ arch wire–bracket combinations. In fact, the contact area determines the probability of getting large wear track exposed to the environment and thereby the chance of consuming more frictional energy resulting in an increase of the frictional force, thus increasing the coefficient of friction. In agreement with our results, Glenys *et al.* (30) reported also that a larger arch wire size may lead to an increase of the coefficient of friction.

Useful information can also be derived from the analysis of worn surfaces. All the wear tracks visible on the arch wires after fretting tests performed under the different set of test conditions considered in this study, contain scratches, grooves, and oxidized layers. Therefore, different wear mechanisms are active in the sliding contacts between bracket and arch wire inducing a competition between abrasive wear and oxidational wear processes.

A zoom-in on the different wear tracks on the arch wires generated during fretting in the different environmental tests, clarifies the damage on the arch wire surfaces. In ambient air of 50% RH (Fig. 7), SEM of the wear tracks on the arch wires reveals grooves and scratches as well as a number of cracks on 0.017″ × 0.025″ and 0.018″ × 0.025″ arch wires. Some oxidized debris are also observed in and around the wear tracks.

Based on the electrochemical results (Fig. 9), a drop in potential and an increase in current noticed once fretting is started, may indicate that the initial surface oxide layer film on top of the arch wire is partially or totally removed (depassivation process). While at the end of fretting, when the bracket is lifted away from the arch wire surface, an inverse behavior of potential and current is observed marking the repassivation process. At that stage, the damaged arch wire surface becomes covered by a freshly formed passive oxide surface film. Such observations were noticed in all test environments used in this study. However, differences were noticed between the potential and current values recorded in the different test solutions. These differences can be related to the nature of the passive oxide film formed in the different solutions depending on the pH value and the composition of each solution.

The highest initial open-circuit potential was noticed in the Ringer solution in comparison with the other solutions, namely the Ringer solutions containing either a buffer or glucose, and Coca Cola®. This may indicate the good quality of the passive formed film in Ringer solutions. The currents recorded before and after the fretting tests were almost at the same level in all cases. This indicates that repassivation takes place after the end of the fretting tests in all tested solutions. In all cases, except Coca Cola®, the current increases sharply on loading of the bracket on the arch wire, then decreases, and remains at a lower level until fretting is ended. But in Coca Cola®, the current increases not only on loading but also during the whole duration of the fretting test and can be explained by its low pH value, which does not promote repassivation of the wear track area.

Conclusions

The frictional behavior of stainless steel arch wire–bracket combinations during fretting tests performed in different test environments was investigated. The highest coefficient of friction was noticed for the 0.018″×0.025″ arch wire–bracket combination in comparison with 0.017″×0.025″ arch wire–bracket combination for all test environments tested, namely ambient air, a Ringer solution, a Ringer solution containing either a buffer or glucose, and Coca Cola®. The lowest coefficient of friction was noticed during fretting tests performed in solutions most probably due to a lubricating effect of the solution in the contact interface, what did not occur in ambient air. The coefficient of friction was found to be independent of the surface roughness of the arch wires used in this study, but could be related to the effect of the arch wire size. The damage on the arch wires induced during *in-vitro* fretting tests is governed by a competition between oxidational wear and abrasive wear process.

References

1. Tselepis M, Brockhurst P, West VC. The dynamic frictional resistance between orthodontic brackets and arch wires. *Am J Orthod Dentofacial Orthop* 1994;**106**:131–8.
2. Kapilla S, Angolkar PV, Duncanson MD, Nanda RS. Evaluation of friction between edgewise stainless steel bracket and orthodontic wires of four alloys. *Am J Orthod Dentofacial Orthop* 1990;**98**:117–26.
3. Willems G, Carels CEL, Verbeke G. In vitro peel/shear bond strength evaluation of orthodontic bracket base design. *J Dent* 1997;**25**:271–8.
4. Kusy RP, Whitley JQ. Effects of sliding velocity on the coefficient of friction in a model orthodontic system. *Br J Orthod* 1989;**5**:235–40.
5. Mohrbacher H, Celis JP, Roos JR. Laboratory testing of displacement and load induced fretting. *Tribology Int* 1995;**28**:269–78.
6. Willems G, Clocheret K, Celis JP, Verbeke G. Frictional behaviour of stainless steel arch wire–bracket combinations subjected to small oscillating displacements. *Am J Orthod Dentofacial Orthop* 2001;**120**:371–7.
7. Waterhouse RB. Fretting wear. *Wear* 1984;**100**:107–18.
8. Loftus BP, Artun J, Nichollas JI. Evaluation of friction during sliding tooth movement in various bracket–archwire combinations. *Am J Orthod Dentofacial Orthop* 1999;**116**:336–45.
9. Ogata RH, Nanda RS, Duncanson MG. Frictional resistances in stainless steel bracket wire combinations with effects of vertical deflections. *Am J Orthod Dentofacial Orthop* 1996;**109**:535–42.
10. Peterson L, Spencer R, Andreasen GF. Comparison of frictional resistance of Nitinol and stainless steel wires in edgewise brackets. *Quintessence Int* 1982;**13**:563–71.
11. Kusy RP, Whitley JQ. Effects of surface roughness on the coefficients of friction in model orthodontic systems. *J Biomech* 1990;**23**:913–25.
12. Kusy RP, Whitley JQ. Influence of archwire and bracket dimension on sliding mechanics: derivations and determinations of the critical contact angle for binding. *Eur J Orthod* 1999;**21**:199–208.
13. Keith O, Jones SP. The influence of bracket material, ligation force and wear on frictional resistance of orthodontic brackets. *Br J Orthod* 1993;**20**:109–15.
14. Riley JL, Garrett SG, Moon PC. A frictional force of ligated plastic and metal edgewise brackets. *J Dent Res* 1979;**58**:98.
15. Moore JC, Waters NE. Factors affecting tooth movement in sliding mechanics. *Eur J Orthod* 1993;**15**:235–41.
16. Baker KL, Nieberg LG, Weimer AD. Frictional changes in force values caused by saliva substitution. *Am J Orthod Dentofacial Orthop* 1987;**91**:316–20.

17. Schlegel V. Relative friction minimization in fixed orthodontic bracket appliances. *J Biomech* 1996;**29**:483–91.
18. Waterhouse B. *Fretting Corrosion*. Oxford: Pergamon Press; 1975.
19. Kusy RP, Whitley JQ. Coefficients of friction for arch wires in stainless steel and polycrystalline alumina brackets slots. *Am J Orthod Dentofacial Orthop* 1990;**98**:300–12.
20. Andreasen GF, Quevedo FR. Evaluation of friction forces in the 0.022″ × 0.028″ edgewise bracket in vitro. *J Biomech* 1970;**3**: 151–60.
21. Downing A, Mccabe J, Gordon PH. The effect of artificial saliva on the frictional forces between orthodontic brackets and arch wires. *Br J Orthod* 1995;**22**:141–6.
22. Rabinowicz E. *Friction and Wear of Materials*. New York: John Wiley & Sons; 1965.
23. Kuzy RP, Whitley JQ, Prewitt JM. Comparison of the frictional coefficients for selected arch wire bracket slot combinations in the dry and wet states. *Angle Orthod* 1991;**61**:293–302.
24. Glenys A, Thorstenson BS, Kusy RP. Resistance to sliding of self-ligation brackets versus conventional stainless steel twin brackets with second-order angulation in the dry and wet (saliva) states. *Am J Orthod Dentofacial Orthop* 2001;**120**: 361–70.
25. Rossouw PE, Kamelchuk LS, Kusy RP. A fundamental review of variables associated with low velocity frictional dynamics. *Semin Orthod* 2003;**9**:223–35.
26. Willems G, Lambrechts P, Braem M, Vuylsteke-Wauters M, Vanherle G. The surface roughness of enamel-to-enamel contact areas compared with intrinsic roughness of dental resin composites. *J Dent Res* 1991;**70**:1299–305.
27. Chimenti C, Lecce D, Santucci L, Parziale V. In vitro assessment of elastometric chain behaviour. *Prog Orthod* 2001;**2**:42–5.
28. Negoro M, Nakagakia H, Tsuboia S, Adachia K, Hanakia M, Tanakaa D, et al. Oral glucose retention saliva viscosity and flow rate in 5-year-old children. *Arch Oral Biol* 2000;**45**:1005–11.
29. Davis JR. Biomaterials for dental applications. In: Davis JR, editor. *Handbook of Materials for Medical Devices*. Ohio: ASM International; 2003. pp 204.
30. Glenys A, Thorstenson BS, Kusy RP. Effect of arch wire size and material on the resistance to sliding of self-ligating brackets with second-order angulation in the dry state. *Am J Orthod Dentofacial Orthop* 2002;**122**:295–305.